# Shapiro steps and stimulated radiation of electromagnetic waves due to Josephson oscillations in layered superconductors

L. N. Bulaevskii
*Los Alamos National Laboratory, Los Alamos, New Mexico 87545, USA*

A. E. Koshelev
*Materials Science Division, Argonne National Laboratory, Argonne, Illinois 60439, USA*

M. Tachiki
*Graduate School of Frontier Sciences, The University of Tokyo, Kashiwanoha 277-8568, Japan*
(Received 24 September 2008; published 19 December 2008)

Single crystals of layered high-temperature superconductors intrinsically behave as stacks of Josephson junctions. We analyze response of current-biased stack of intrinsic junctions to irradiation by the external electromagnetic (em) wave. In addition to well-known Shapiro steps in the current-voltage characteristics, irradiation promotes stimulated radiation which adds with spontaneous Josephson radiation from the crystal. Such enhancement of radiation from current-biased crystal may be used for amplification of em waves. Irradiation also facilitates synchronization of Josephson oscillations in all intrinsic Josephson junctions of a single crystal as well as oscillations in intrinsic junctions of different crystals.

DOI: 10.1103/PhysRevB.78.224519 PACS number(s): 85.25.Cp, 74.50.+r, 42.25.Gy

## I. INTRODUCTION

Use of Josephson coupled cuprate superconductors such as $Bi_2Sr_2CaCu_2O_8$ (BSCCO) for generation and detection of electromagnetic (em) radiation in the terahertz frequency range is in the focus of many recent experimental and theoretical studies both in zero external magnetic field[1–7] and for the moving Josephson vortex lattice.[8–12] With respect to radiation, the goal is to get powerful, tunable, and coherent terahertz electromagnetic radiation due to synchronized Josephson oscillations in many intrinsic Josephson junctions (IJJs) biased with the direct $c$-axis current. Due to very high density of IJJs along the $c$ axis in BSCCO crystals, it is possible to obtain strong emittance from the crystal edge into free space in the super-radiation regime.[7] Such a radiation enhances the direct current at a given voltage because radiation results in effective dissipation of energy from the junction edges in addition to that caused by quasiparticles inside the junctions. The opposite effect, Shapiro step in the $c$-axis current-voltage ($I$-$V$) characteristic at given voltage due to irradiation of the crystal by the em wave, provides basis for detection of the terahertz radiation by layered superconductors.

The Shapiro steps in IJJ were observed without applying magnetic field[1–3,13–16] and also in the moving vortex lattice state.[9] Step formation is usually discussed using approach outlined in the pioneering works of Josephson and of Shapiro. In this approach the amplitudes of dc and ac voltages ($V$ and $v$) are assumed to be fixed leading to modulation the frequency of the Josephson current via the junction,

$$\omega(t) = (2e/\hbar)[V + v\cos(\Omega t + \beta)], \tag{1}$$

where $\Omega$ is the external frequency. At the matching conditions $\omega_J = 2eV/\hbar = n\Omega$ with $n = 1, 2, \ldots$, such frequency modulations lead to the dc components in the Josephson current,

$$\langle I(t)\rangle_t = I_c\left\langle \sin\left[\int_0^t d\tau\omega(\tau) + \beta_0\right]\right\rangle_t = I_c(-1)^n J_n\left(\frac{2ev}{\hbar\Omega}\right)\sin(\beta_0 - n\beta), \tag{2}$$

where $J_n(x)$ is the Bessel function. One can see from this expression that the Shapiro steps result from adjustment of the phase of Josephson oscillations to the bias current at given phase of external ac voltage. Heights of these Shapiro steps are determined by the Bessel function $J_n(2ev/\hbar\Omega)$. In more quantified description the alternating external current $I_{\rm ext}\cos(\Omega t + \beta)$, rather than ac voltage, is assumed to be fixed. This current has to be introduced in the right-hand side of the sine-Gordon equation for the phase difference to obtain the amplitude of the induced alternating current voltage $v$.[17] To convert external em wave into the alternating current inside IJJ and, finally, into the direct current, antenna sensitive to the external ac electric field $\mathbf{E}_e$ was used.[2,3] At small incident powers the amplitude of the induced ac voltage scales as the square root of the incident-wave power, $v \propto \sqrt{P}$.

Josephson junctions in resistive state emit electromagnetic radiation. In addition to forming the Shapiro step, the external irradiation also modifies this generated radiation. In particular, in the region of current enhancement, $\langle I(t)\rangle_t > 0$, the irradiation promotes conversion of dc power into the additional stimulated radiation. The key feature of this stimulated radiation is that its power is proportional to the square root of the incident power. The relation between the first Shapiro step, $n = 1$, and radiation from IJJ will be the focus of this paper.

First, we note that the conversion of incident em wave into extra direct current (Shapiro step) inside layered superconductors with IJJ may be realized not only by use of an-

 

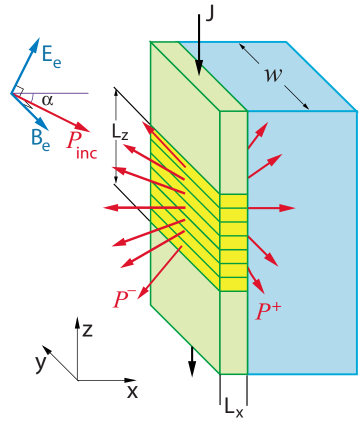


FIG. 1. (Color online) Schematic picture of a layered superconductor cut in the form of layer stack (in the middle) and screens. The directions of the transport direct current, $J$, of the incident wave, $P_{\rm inc}$ are shown. The incident em wave induces the oscillating $c$-axis current in the crystal. Interaction of this current with the Josephson oscillations leads to the Shapiro step in the current-voltage dependence and stimulates additional backward and forward radiations, $\mathcal{P}^-$ and $\mathcal{P}^+$.

tenna external to the crystal [crystal-antenna (CA) channel][1–3,5,16] but also via direct irradiation of the crystal edge parallel to the $ac$ or $bc$ plane [direct-irradiation (DI) channel].[9,15] Coupling of external em field and the em field inside the junctions at the crystal edge is described by the Maxwell boundary conditions which relate incident em wave directly to the phase differences at IJJ edges. For DI channel the crystal itself plays the role of antenna. We will derive the Shapiro step and radiation power for such DI setup and we will show that overall radiation from the crystal increases (decreases) when the current at the Shapiro step increases (decreases) with respect to that in the absence of irradiation. We will also find the conditions for zero-crossing Shapiro steps in the case of direct irradiation.[3,15]

We note that CA and DI channels are optional also for the transmission of the em wave when Josephson oscillations in IJJ are used to convert the interlayer direct current into the em waves. Layered crystal may be used as a transmitter in the design CA (Ref. 5) or it may directly emit the em waves into the free space from crystal edge as described in Refs. 7 and observed in Ref. 6. It is the latter channel which makes possible tunable super-radiation from large number $N$ of IJJ with high power proportional to $N^2$.

We consider crystal with sizes $L_x$, $w$, and $L_z=Ns$ in the directions $x$, $y$, and $z$, respectively (see Fig. 1). We assume that (i) $L_x, L_z \lesssim \lambda_\omega/2 = c/(2\omega_J)$, (ii) $w \gg \lambda_\omega$ and incident wave has wave vector $\mathbf{k}=(k_x,0,k_z)$ so that all quantities may be assumed $y$ independent, and (iii) JJ stack is bounded by metallic contacts with the same lateral sizes as the stack and extends in the $z$ direction over distance $L_{\rm sc}/2 \gg \lambda_\omega$. We assume that the contact material has a very small surface impedance. Such contacts serve as a screens restricting radiation to half-infinite spaces $|x| > L_x/2$ and thus preventing destructive interference of radiation from the edges $x = \pm L_x/2$ of the crystal. The right half-space is filled by a dielectric with the permeability $\epsilon_d$.

We consider the incident plane wave coming from left half-space. The components of this wave with nonzero $E_x$ and $E_y$ are reflected back due to superconducting currents along the layers. The only part of the wave with polarization such that $E_z \neq 0$ interacts with the Josephson currents and leads to the Shapiro steps and re-emission into left and right half-spaces. To find the $I$-$V$ characteristics we need to match the em fields outside and inside the crystal.

Inside the junction $n$ (between layers $n$ and $n+1$) the average electric field $E_{z,n}$ and magnetic field $B_{y,n}$ are expressed via the phase difference $\varphi_n(x,t)$ as[18]

$$E_{z,n} = (B_c \ell / \sqrt{\epsilon_c})(\partial \varphi_n / \partial \tau), \tag{3}$$

$$(\nabla_n^2 - \ell^{-2} \hat{T}_{ab}) h_{y,n} + \hat{T}_{ab} \nabla_u \varphi_n = 0, \tag{4}$$

and the equation for $\varphi_n(x,t)$ is

$$\frac{\partial^2 \varphi_n}{\partial \tau^2} + \nu_c \frac{\partial \varphi_n}{\partial \tau} + \sin \varphi_n - \nabla_u h_{y,n} = 0. \tag{5}$$

Here $h_{y,n}=B_{y,n}/B_c$ with $B_c=\Phi_0/(2\pi\lambda_{ab}\lambda_c)$ and $\hat{T}_{ab} \equiv 1 + \nu_{ab}\partial/\partial\tau$. We use reduced $x$ coordinate, $u=x/\lambda_J$, normalized to $\lambda_J=\gamma s$ and reduced time, $\tau=\omega_p t$, and $\omega=\omega_J/\omega_p$, where $\omega_p=c/(\lambda_c\sqrt{\epsilon_c})$ is the plasma frequency, $\epsilon_c$ is the $c$-axis high-frequency dielectric constant inside the superconductor, $\lambda_{ab}$ and $\lambda_c$ are the London penetration lengths, $\gamma=\lambda_c/\lambda_{ab}$ is the anisotropy ratio, $\ell \equiv \lambda_{ab}/s$, and $\nabla_n^2$ notates the discrete second derivative operator, $\nabla_n^2 A_n = A_{n+1} + A_{n-1} - 2A_n$. We neglected capacitive coupling[19] because it does not affect our results (see Ref. 7). In terms of these parameters the Josephson critical current is $J_c=\Phi_0 c/(8\pi^2 s \lambda_c^2)$. The dissipation parameters, $\nu_{ab}=4\pi\sigma_{ab}/(\gamma^2\epsilon_c\omega_p)$ and $\nu_c=4\pi\sigma_c/(\epsilon_c\omega_p)$, are determined by the quasiparticle conductivities, $\sigma_{ab}$ and $\sigma_c$, along and perpendicular to the layers, respectively. The typical parameters of the optimally doped BSCCO at low temperatures[20] are $\epsilon_c=12$, $s=15.6$ Å, $\gamma=500$, $\lambda_{ab}=200$ nm, $J_c=1700$ A/cm$^2$, $\sigma_c(0)=2\times10^{-3}$ $(\Omega\ \mathrm{cm})^{-1}$. This gives $\ell \approx 130$ and $\nu_c \approx 2\times10^{-3}$.

External and internal em fields are related via the Maxwell boundary conditions, i.e., continuity of the transverse field components across the boundary. These conditions, according to Eqs. (3) and (4), provide also the boundary conditions for the phase differences, i.e., the relations between time and space derivatives of $\varphi_n(x,t)$ at the edges. They allow us to solve Eqs. (4) and (5) for $\varphi_n(x,t)$ and find the $I$-$V$ characteristics, the Shapiro steps, and the Poynting vector of radiation.

## II. BOUNDARY CONDITIONS FOR FIELDS

We formulate the boundary conditions at the edges parallel to $(y,z)$. As the $y$ and $z$ sizes of the system (crystal and screens) are assumed to be larger than the wavelength, the electromagnetic wave fields can be considered $y$ independent and the spaces to the left and to the right from screens and crystal may be treated as half-infinite. In the case of such half-infinite space geometry for propagating waves we find the boundary conditions analytically. From the Maxwell equations in the free space we find relation between the magnetic, $\mathbf{B}=(0,B_y,0)$, and the electric, $\mathbf{E}=(E_x,0,E_z)$, fields at the boundaries. The electromagnetic field in the left half-space consists of the incident plane wave with the fields,

$$E_{z,e}=-B_{y,e}\cos\alpha,\quad E_{x,e}=B_{y,e}\sin\alpha,$$

$$B_{y,e}=B_e\exp\{i[k_{\omega,x}(x+L_x/2)+k_{\omega,z}z+\beta-\omega\tau]\},$$

where $(k_{\omega,x},k_{\omega,z})=(k_\omega\cos\alpha,k_\omega\sin\alpha)$, and outgoing radiated and reflected electromagnetic waves propagating from the crystal in all directions in the $(x,z)$ plane,

$$B_{y,r},E_{x,r},E_{z,r}\propto\exp\{-i[k_x(x+L_x/2)+k_zz+\omega\tau]\},$$

where $k_x=\mathrm{sgn}(\omega)(k_\omega^2-k_z^2)^{1/2}$ for $k_z^2<k_\omega^2$ and $k_x=i(k_z^2-k_\omega^2)^{1/2}$ for $k_z^2>k_\omega^2$. Here $\alpha$ is the propagation angle, $k_\omega=\omega/c$ and $\beta$ is the phase of the incident wave at the crystal edge relative to the phase of Josephson oscillations inside the junctions. The em wave propagating backward is composed from the plane wave reflected from the screens and cylindrical waves reflected and emitted from the crystal area. In terms of the incident and radiated fields the boundary conditions at $u=-\tilde{L}_x/2$ ($\tilde{L}_x=L_x/\lambda_J$) follow from Eqs. (3) and (4) where

$$B_y(n,\alpha)=B_{y,r}(n)+B_{y,e}(n,\alpha),\tag{6}$$

$$E_z(n,\alpha)=E_{z,r}(n)+E_{z,e}(n,\alpha).\tag{7}$$

Here $B_{y,r}(n)$ and $E_{z,r}(n)$ are the emitted em fields at the edge of junction $n$. On the right side, radiated waves are propagating in the dielectric and here we need to replace $k_\omega^2$ in the above expressions by $\epsilon_d k_\omega^2$ and put $B_{y,e}=E_{z,e}=0$ (we do not account for the waves reflected from other side of the dielectric).

The relations between radiated fields at $u=\pm\tilde{L}_x/2$ are[4]

$$B_{y,r}(\omega,k_z)=\mp\zeta_\omega(k_z)E_{z,r}(\omega,k_z),$$

$$\zeta_\omega(k_z)=\begin{cases}\epsilon_\mp|k_\omega|(\epsilon_\mp k_\omega^2-k_z^2)^{-1/2} & \text{for } k_z^2<\epsilon_\mp k_\omega^2\\ -i\epsilon_\mp k_\omega(k_z^2-\epsilon_\mp k_\omega^2)^{-1/2} & \text{for } k_z^2>\epsilon_\mp k_\omega^2.\end{cases}\tag{8}$$

Here we denote $\epsilon_-=1$ and $\epsilon_+=\epsilon_d$.

The inverse Fourier transform with respect to $k_z$ gives nonlocal relations between radiated fields at the edges,

$$\begin{aligned}B_{y,r}(z)&=\int_{-\infty}^{\infty}dz'K_-(z-z')E_{zr}(z')\\&\approx\int_{-L_z/2}^{L_z/2}dz'K_-(z-z')E_z(z')\\&\quad-\int_{-\infty}^{\infty}dz'K_-(z-z')E_{z,e}(z')\\&=\int_{-L_z/2}^{L_z/2}dz'K_-(z-z')E_z(z')+B_{y,e}(z).\end{aligned}$$

Here

$$K_\pm(z)=\frac{\epsilon_\pm}{2}[|k_\omega|J_0(\sqrt{\epsilon_\mp}|k_\omega|z)+ik_\omega N_0(\sqrt{\epsilon_\mp}|k_\omega|z)],\tag{9}$$

with $J_0(x)$ and $N_0(x)$ being the Bessel functions. In the first integral in the second line for $E_z(z')$ we replace infinite limits with $\pm L_z/2$ because the electric field on the surface of screens is very small and the integral outside of screens can be neglected because the kernel $K_-(z-z')$ is small there. The integral over $E_{z,e}(z)$ was transformed using relation

$$\begin{aligned}&-\int_{-\infty}^{\infty}dz'K_-(z-z')E_{z,e}(z')\\&=-\frac{|k_\omega|}{\sqrt{k_\omega^2-k_{\omega,z}^2}}E_{z,e}e^{ik_{\omega,z}z}=B_{y,e}e^{ik_{\omega,z}z}.\end{aligned}$$

Using $B_{y,r}(z)=B_y(z)-B_{y,e}(z)$, we finally derive boundary condition relating the fields at the left side,

$$\begin{aligned}B_y(-L_x/2,z)&=\int_{-L_z/2}^{L_z/2}dz'K_-(z-z')E_z(-L_x/2,z')\\&\quad+2B_{y,e}(-L_x/2,z).\end{aligned}\tag{10}$$

Similarly, for the right side we derive

$$B_y(L_x/2,z)=-\int_{-L_z/2}^{L_z/2}dz'K_+(z-z')E_z(L_x/2,z').\tag{11}$$

These conditions together with Eqs. (3)–(5) determine oscillating phase $\varphi(x,t)$ inside and radiation outside.

### III. SOLUTION FOR OSCILLATING PHASE

In the regime when all junctions are similar and they are irradiated similarly, phases of oscillations in all junctions should be the same as the same $c$-axis direct current flows via all junctions, and oscillations are locked by the irradiation field. We consider high-frequency regime, $\omega=\omega_J/\omega_p\gg 1$, when Shapiro steps may be observed.[21] The equation for uniform phase differences $\varphi_n(u,\tau)=\varphi(u,\tau)$ is

$$\frac{\partial^2\varphi}{\partial\tau^2}+\nu_c\frac{\partial\varphi}{\partial\tau}+\sin\varphi-\ell^2\nabla_u^2\varphi=0.$$

In the limit $\omega\gg 1$ we look for the solution in the form $\varphi(u,\tau)=\omega\tau+\mathrm{Im}[\phi_\omega(u)\exp(-i\omega\tau)]$ where the oscillating part, $\phi_\omega(u)$, is small and satisfies the equation

$$(\omega^2+i\nu_c\omega)\phi_\omega+\ell^2\nabla_u^2\phi_\omega=-1.\tag{12}$$

From Eqs. (10) and (11), using relations $B_y=B_c\ell^2\nabla_u\phi_\omega$ and $E_z=-i\omega(B_c\ell/\sqrt{\epsilon_c})\phi_\omega$, we derive the boundary conditions for $\phi_\omega$. At $u=-\tilde{L}_x/2$ we get

$$\nabla\phi_{\omega,n}=-\frac{is\omega}{\ell\sqrt{\epsilon_c}}\sum_m K_-(k_\omega s|n-m|)\phi_{m,\omega}+\tilde{h},\tag{13}$$

with $\tilde{h}=2h_ee^{i\beta}/\ell^2$ and $h_e=B_e/B_c$. We assume that $k_\omega L_z\sin\alpha\ll 1$ which allow us to neglect $z$ dependence of $B_{y,e}(-L_x/2,z)$ in Eq. (10). Similarly, the boundary condition for $u=\tilde{L}_x/2$ is given by Eq. (13) with $\tilde{h}=0$ and substitute

$K_- \to K_+$. For the case of homogeneous phase, performing summation over $m$, we write the boundary conditions in a simple form,

$$\nabla_u \phi_\omega = -i\omega\zeta_- \phi_\omega + \tilde{h} \quad \text{at} \quad u = -\tilde{L}_x/2,$$

$$\zeta_- = \frac{L_z}{2\ell\sqrt{\epsilon_c}}[|k_\omega| - ik_\omega \mathcal{L}_\omega^{(-)}], \quad \mathcal{L}_\omega^{(-)} \approx \frac{2}{\pi}\ln\left[\frac{5.03}{|k_\omega|L_z}\right], \tag{14}$$

and

$$\nabla_u \phi_\omega = i\omega\zeta_+ \phi_\omega \quad \text{at} \quad u = \tilde{L}_x/2,$$

$$\zeta_+ = \frac{\epsilon_d L_z}{2\ell\sqrt{\epsilon_c}}[|k_\omega| - ik_\omega \mathcal{L}_\omega^{(+)}], \quad \mathcal{L}_\omega^{(+)} \approx \frac{2}{\pi}\ln\left[\frac{5.03}{\sqrt{\varepsilon_d}|k_\omega|L_z}\right]. \tag{15}$$

The solution of Eq. (12) is given by

$$\phi_\omega(u) = -\frac{1}{\omega^2 + i\omega\nu_c} + A\cos(\bar{k}_\omega u) + C\sin(\bar{k}_\omega u), \tag{16}$$

with $\bar{k}_\omega = \sqrt{\omega^2 + i\nu_c\omega}/\ell \approx (\omega + i\nu_c/2)/\ell$. The first term here is the amplitude of uniform Josephson oscillations, while the second and the third terms describe the electromagnetic waves propagating inside the junctions. They are generated at the crystal boundaries due to the radiation fields. The constants $A$ and $C$ have to be found from boundary conditions (14) and (15). Approximately, they can be represented as

$$A \approx [(i\bar{k}_\omega/\omega)\zeta\cos\eta + \tilde{h}(\bar{k}_\omega\cos\eta - i\omega\zeta_+\sin\eta)]\mathcal{D}^{-1},$$

$$C \approx \tilde{h}(\bar{k}_\omega\sin\eta + i\omega\zeta_+\cos\eta)\mathcal{D}^{-1},$$

$$\mathcal{D} \approx \bar{k}_\omega^2\sin(2\eta) + i\bar{k}_\omega\omega\zeta\cos(2\eta). \tag{17}$$

Here $\eta = \bar{k}_\omega\tilde{L}_x/2 \approx (\omega + i\nu_c/2)L_x/(2\lambda_c)$ and $\zeta = \zeta_+ + \zeta_-$, with $|\zeta_\pm| \ll 1$. We kept only terms lowest in order $1/\ell \ll 1$. In the following we will mostly focus on the case of narrow stack, $\omega L_x/\lambda_c \ll 1$. In this limit one can neglect coordinate dependence of the oscillating phase inside the stack leading to a very simple analytical result

$$\phi_\omega(u) \approx -\frac{\tilde{L}_x - \tilde{h}\ell^2}{(\omega^2 + i\nu_c\omega)\tilde{L}_x + i\omega\ell^2\zeta}. \tag{18}$$

It was shown in Ref. 7 that without external radiation the homogeneous synchronized state is stable with respect to small perturbations due to interaction with generated radiation field in combination with intralayer dissipation.[22] Interaction with the radiation field also synchronizes oscillation in different junctions in slightly inhomogeneous system.[7] Irradiation field certainly enhances stability of uniform oscillations and synchronization in inhomogeneous system. Quantitatively, these effects will be considered elsewhere. In the following we will use results [Eqs. (17) and (18)] to evaluate the height of Shapiro step in the current-voltage characteristic and radiation powers in the forward and backward directions.

## IV. FIRST SHAPIRO STEP

We proceed now with derivation of the $I$-$V$ characteristic and power of radiation from the irradiated crystal. In the first order in $\phi_\omega$ ($n=1$ Shapiro step) the dimensionless dc current density $j = J/J_c$ is given by the expression $j = \nu_c\omega + \langle \mathrm{Im}[\phi_\omega]\rangle/2$. The total dc interlayer current density consists of the quasiparticle contribution, $j_{\mathrm{qp}}$, the current induced by radiation in the absence of incident wave,[7] $j_{\mathrm{sp}}$, and also irradiation-induced (stimulated) current $j_{\mathrm{stim}}$,

$$j = j_{\mathrm{qp}} + j_{\mathrm{sp}} + j_{\mathrm{stim}}(\beta), \quad j_{\mathrm{qp}} = \nu_c\omega + \frac{\nu_c}{2\omega^2}, \tag{19}$$

$$j_{\mathrm{sp}} = \frac{a}{2\omega^2\mathcal{G}^2}, \tag{20}$$

$$j_{\mathrm{stim}}(\beta) \approx \frac{h_e}{\ell^2}\mathrm{Im}\left[\frac{\exp(i\beta)\sin(2\eta)/(2\eta)}{\bar{k}_\omega\sin(2\eta) + i\omega\zeta\cos(2\eta)}\right], \tag{21}$$

with

$$\mathcal{G}^2 = (1 + \mathcal{L}_\omega a)^2 + a^2, \quad a = \frac{L_z(1+\epsilon_d)}{2L_x\epsilon_c},$$

and $\mathcal{L}_\omega = (\mathcal{L}_\omega^{(-)} + \epsilon_d\mathcal{L}_\omega^{(+)})/(1+\epsilon_d)$. The second term, $j_{\mathrm{sp}}$, corresponding to spontaneous radiation, becomes significant at large $N$ as the effectiveness of direct channel increases with $N$ (while the effectiveness of antenna channel in the design crystal antenna decreases with $N$ as impedance of the crystal increases with $N$). As a result, large-$N$ crystal may work effectively as a transmitter as well as a receiver without external antenna.

The Shapiro-step term, $j_{\mathrm{stim}}(\beta) \propto B_e$, is the current due to the stimulated radiation. In the limit $\nu_c \ll \omega$ and in the narrow-stack regime, $\omega L_x/\lambda_c \ll 1$, we expand it in small $\eta$ and, using $\omega\zeta/(2\bar{k}_\omega\eta) \approx \ell\zeta/(2\eta) \approx a[1 - i\mathcal{L}_\omega]$, we obtain

$$j_{\mathrm{stim}} \approx \frac{B_e\lambda_J}{B_c L_x\omega^2\mathcal{G}}\sin(\beta - \beta_0), \quad \tan\beta_0 = \frac{a}{\mathcal{L}_\omega a + 1}. \tag{22}$$

The current $j_{\mathrm{stim}}(\beta)$ may take any value in the interval $[-j_{\mathrm{step}}/2, j_{\mathrm{step}}/2]$ as the phase $\beta$ adjusts to a given value of total current $j \geq 0$ in the interval $-\pi/2 < \beta - \beta_0 < \pi/2$ at fixed voltage [see Fig. 2(a)]. The full Shapiro-step height is given by the expression

$$j_{\mathrm{step}} = \frac{2B_e\lambda_J}{B_c\omega^2 L_x\mathcal{G}}. \tag{23}$$

The step amplitude weakly depends on the number of resistive junctions $N$ for $N < 2L_x\epsilon_c/[s(1+\epsilon_d)]$ and decreases as $N^{-2}$ for larger $N$. For the total current, $I_{\mathrm{step}} = J_c L_x w j_{\mathrm{step}}$, we estimate the Shapiro-step height for BSCCO at $\omega/2\pi = 1$ THz as $I_{\mathrm{step}}/(wB_e) \approx 30$ mA/(cm G) in the case of short mesa, $N=10$, $L_x = 10$ $\mu$m. For tall mesa, $L_z = 40$ $\mu$m and

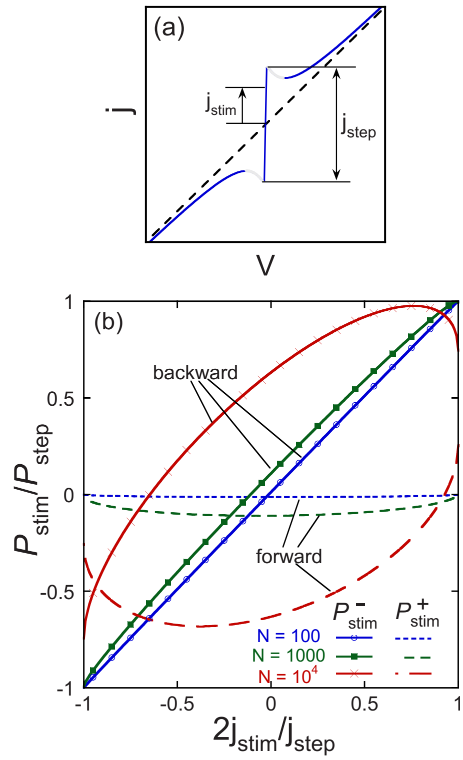


FIG. 2. (Color online) (a) Schematic of Shapiro step in the current-voltage dependence. (b) Representative dependences of the stimulated radiation powers in forward and backward directions on the Shapiro-step current for different numbers of junctions in the stack. We used parameters $\omega/2\pi=1$ THz, $L_x=10$ $\mu$m, $\epsilon_c=12$, and $\epsilon_d=10$.

$L_x=4$ $\mu$m, we estimate $I_{\text{step}}/(wB_e)\approx 10$ mA/(cm G). The latter geometry is close to the optimal one for radiation[7] and such a crystal may work effectively for both transmission and detection.

Zero-crossing Shapiro step occurs when $j=0$. This is possible if $\omega \gg 1$ and if spontaneous radiation is small. For small $N$, when $a \ll 1$, $\nu_c\omega^3$, such a radiation may be neglected. Then the condition for zero-crossing Shapiro step, $j_{\text{step}}/2 \geq \nu_c\omega$, can be represented as

$$B_e \geq \nu_c B_c \frac{L_x}{\lambda_J}\frac{\omega^3}{\omega_p^3}. \tag{24}$$

At given $V>0$ and positive currents the battery power is converted into heat due to quasiparticle dissipation and also into radiation, as we will show in Sec. V. At negative currents irradiation power is converted into heat and into direct current which charges the battery as $IV<0$ there.[23]

## V. STIMULATED RADIATION

In this section we analyze radiation emitted from the stack in both directions in the form of cylindrical waves. The Poynting vector of the radiation into the right side is given by the expression

$$\mathcal{P}_x^+ = \frac{c\omega^2 B_c^2 \ell^3}{8\pi\sqrt{\varepsilon_c}}\text{Re}[\zeta_+]|\phi_\omega(L_x/2)|^2. \tag{25}$$

In the limits $\nu_c \ll \omega$ and $\omega L_x/\lambda_c \ll 1$ we can evaluate $\mathcal{P}_x^+$ using Eq. (18). The total Poynting vector can be split naturally into three contributions,

$$\mathcal{P}_x^+ = \mathcal{P}_{x,\text{sp}}^+ + \mathcal{P}_{x,\text{stim}}^+ + \mathcal{P}_{x,n}^+, \tag{26}$$

with

$$\mathcal{P}_{x,\text{sp}}^+ \equiv \mathcal{P}_{x0}^+ = \frac{\pi\epsilon_d J_c^2 L_z}{\epsilon_c^2\omega_J \mathcal{G}^2}, \tag{27}$$

$$\mathcal{P}_{x,\text{stim}}^+ = -\mathcal{P}_{x0}^+\frac{4B_e\lambda_J}{B_cL_x}\cos\beta, \tag{28}$$

$$\mathcal{P}_{x,n}^+ = \frac{cB_e^2}{4\pi}\frac{\epsilon_d L_z c}{\epsilon_c^2\omega_J\mathcal{G}^2 L_x^2}. \tag{29}$$

The term $\mathcal{P}_{x,n}^+$ is not affected by Josephson oscillations and it describes the transmitted wave in the absence of the bias current. The spontaneous radiation power in the absence of an incident wave, $\mathcal{P}_{x0}^+ \equiv \mathcal{P}_x(\tilde{h}=0)$, corresponds to the second term in the right-hand side of Eq. (19) and it was discussed in Ref. 7. For small $L_x$, $L_x \ll L_z/\epsilon_c$, $\mathcal{P}_{x,\text{sp}} \propto L_x^2$, and it is $N$ independent, while for larger $L_x$, in the super-radiation regime, it is proportional to $N$ and is independent of $L_x$. The radiation intensity depends on the angle of propagation $\theta$ with respect to the $x$ axis as $\cos\theta$.

The total energy-flow density at the left side, $P_x^-$, is given by

$$P_x^- = -\frac{cB_c^2\ell^3\omega}{8\pi\sqrt{\epsilon_c}}(\omega\,\text{Re}[\zeta_-]|\phi_\omega^-|^2 - \text{Im}[\phi_\omega^{-*}\tilde{h}]), \tag{30}$$

with $\phi_\omega^- = \phi_\omega(-L_x/2)$. The reflected power density, $\mathcal{P}_x^-$, is related to $P_x^-$ as $P_x^- = \frac{cB_e^2}{8\pi} - \mathcal{P}_x^-$. Using again Eq. (18), we derive

$$\mathcal{P}_x^- = \mathcal{P}_{x,\text{sp}}^- + \mathcal{P}_{x,\text{stim}}^- + \mathcal{P}_{x,n}^-, \tag{31}$$

$$\mathcal{P}_{x,\text{sp}}^- \equiv \mathcal{P}_{x0}^- = \frac{\pi J_c^2 L_z}{\epsilon_c^2\omega_J\mathcal{G}^2}, \tag{32}$$

$$\mathcal{P}_{x,\text{stim}}^- = \mathcal{P}_{x0}^-\frac{2B_e\lambda_J}{B_cL_x}\left[\frac{(\epsilon_d+1)\sin\beta}{\tan\beta_0} + (\epsilon_d-1)\cos\beta\right], \tag{33}$$

$$\mathcal{P}_{x,n}^- = \frac{cB_e^2}{8\pi}\left(1 - \frac{2\epsilon_d L_z}{\epsilon_c^2 k_\omega L_x^2\mathcal{G}^2}\right). \tag{34}$$

We can check that the derived radiation powers satisfy the energy conservation law,

$$\mathcal{P}_x^+ + \mathcal{P}_x^- = (j_{\text{sp}} + j_{\text{stim}})J_c\frac{L_xV}{s} + \frac{cB_e^2}{8\pi}, \tag{35}$$

where $V$ is the voltage drop per single junction.

A natural scale for the stimulated radiation is given by the extra power at the Shapiro step provided by dc source,

$$\mathcal{P}_{\text{step}} = J_c L_x \frac{V}{s} \frac{j_{\text{step}}}{2},$$

where the Shapiro-step height $j_{\text{step}}$ is given by Eq. (23). Using this scale, we can rewrite results for $\mathcal{P}^{\pm}_{x,\text{stim}}$ in a more transparent form,

$$\mathcal{P}^{+}_{x,\text{stim}} = -\mathcal{P}_{\text{step}} \frac{2\epsilon_d}{\epsilon_d + 1} \sin\beta_0 \cos\beta, \tag{36}$$

$$\mathcal{P}^{-}_{x,\text{stim}} = \mathcal{P}_{\text{step}} \left[ \cos\beta_0 \sin\beta + \frac{\epsilon_d - 1}{\epsilon_d + 1} \sin\beta_0 \cos\beta \right]. \tag{37}$$

Both $j_{\text{stim}}$ and the total stimulated radiation power reach maximum when $\beta = \pi/2 + \beta_0$, i.e., at the highest point of the Shapiro step. Split of the total power between the forward and backward directions depends mostly on the aspect ratio of the stack. The representative dependences of the stimulated radiations in transmission and in reflection on the Shapiro-step current $j_{\text{stim}}$ for different $N$ are shown in Fig. 2(b). The stimulated contribution decreases the total radiation at $j_{\text{stim}} < 0$, while at $j_{\text{stim}} > 0$, the radiation increases predominantly in the backward direction. At $a \ll 1$ (for small $N \ll 2L_x\epsilon_c/[s(1+\epsilon_d)]$) the forward stimulated radiation is negligible, while the Poynting vector of the backward radiation becomes proportional to stimulated current,

$$\mathcal{P}^{-}_{x,\text{stim}} = \frac{L_x V}{s} J_c j_{\text{stim}} \tag{38}$$

[see, e.g., plots for $N = 100$ in Fig. 2(b)]. In this limit almost all stimulated current is converted into the backward radiation at $j_{\text{stim}} > 0$, while at $j_{\text{stim}} < 0$ the radiation losses are reduced by the amount proportional to $|\mathcal{P}^{-}_{x,\text{stim}}|$, decreasing the power consumption from the battery. The external radiation may even charge the external battery in the case of the zero-crossing Shapiro step.

The effect of enhancement of the radiation at $\sin(\beta - \beta_0) > 0$, in principle, may be used to amplify the electromagnetic waves. In the terahertz frequency range enhancement of the Pointing vector $\mathcal{P}_x$ at the maximum point $\beta = \pi/2 + \beta_0$ is given by Eq. (31). We estimate that for realistic powers of the external wave the maximum stimulated power density always exceeds external power density. Moreover, for sufficiently large external power, at $B_e > B_c(1+\epsilon_d)L_z/(4\epsilon_c \mathcal{G}\lambda_J)$, the stimulated radiation may also have larger power than the spontaneous radiation. For example, unirradiated crystal with $L_x = 4$ $\mu$m in the super-radiation regime, $L_z = 40$ $\mu$m, emits the em wave with the amplitude $B_{r,y} \approx 3.5 B_c \approx 0.6$ G corresponding to the power density $\sim 40$ W/cm$^2$. Irradiation of such crystal with external wave with the same power would generate maximum stimulated radiation with six times larger power.

## VI. CONCLUSIONS

In conclusion, we considered the response of the IJJ stack in the resistive state to external irradiation with the frequency coinciding with the Josephson frequency. Irradiation of $c$-axis dc-biased layered crystal leads to additional stimulated radiation from the crystal at the upper part of the Shapiro step. Both Shapiro-step current and stimulated radiation are determined by the phase shift between the incident electromagnetic wave and Josephson oscillations. During current sweep, this phase shift is adjusted to the value of current. At the lower part of the Shapiro step with zero-crossing current the power of the incident em wave is converted into dc charging the battery. The setup shown in Fig. 1, in principle, may be used as an amplifier of the em waves in the terahertz frequency range. The important role of external radiation is that it also enforces the synchronization of Josephson oscillations in all junctions of a crystal and fixes the phase of radiated electromagnetic wave. In the same way one can synchronize radiation from several crystals. Even though our quantitative analysis is only valid for specific simplified geometry, we expect that similar stimulated radiation should also exist in other geometries. Up to now only formation of the Shapiro steps by external radiation in the current-voltage dependences has been studied. It would be very interesting to perform combined analysis of both transport and outgoing radiation in the Shapiro-step region.

## ACKNOWLEDGMENTS

The authors thank I. Martin for useful discussions. The research was supported by the U.S. DOE under the Contracts No. W-7405-Eng-36 (LANL) and No. DE-AC02-06CH11357 (ANL).

---

[1] G. Hechtfischer, W. Walkenhorst, G. Kunkel, K. Schlenga, R. Kleiner, P. Müller, and H. L. Johnson, IEEE Trans. Appl. Supercond. **7**, 2723 (1997).

[2] S. Rother, Y. Koval, P. Müller, R. Kleiner, Y. Kasai, K. Nakajima, and M. Darula, IEEE Trans. Appl. Supercond. **11**, 1191 (2001).

[3] H. B. Wang, P. H. Wu, and T. Yamashita, Phys. Rev. Lett. **87**, 107002 (2001).

[4] L. N. Bulaevskii and A. E. Koshelev, J. Supercond. Novel Magn. **19**, 349 (2006).

[5] I. E. Batov, X. Y. Lin, S. V. Shitov, Y. Koval, P. Müller, and A. V. Ustinov, Appl. Phys. Lett. **88**, 262504 (2006).

[6] L. Ozyuzer, A. E. Koshelev, C. Kurter, N. Gopalsami, Q. Li, M. Tachiki, K. Kadowaki, T. Yamamoto, H. Minami, H. Yamaguchi, T. Tachiki, K. E. Gray, W. K. Kwok, and U. Welp, Science **318**, 1291 (2007).

[7] L. N. Bulaevskii and A. E. Koshelev, Phys. Rev. Lett. **99**, 057002 (2007); A. E. Koshelev and L. N. Bulaevskii, Phys. Rev. B **77**, 014530 (2008).

[8] T. Koyama and M. Tachiki, Solid State Commun. **96**, 367

(1995).
[9] Yu. I. Latyshev, M. B. Gaifullin, T. Yamashita, M. Machida, and Y. Matsuda, Phys. Rev. Lett. **87**, 247007 (2001); M. B. Gaifullin, Yu. I. Latyshev, T. Yamashita, and Y. Matsuda, Physica C **392-396**, 319 (2003).
[10] M. Tachiki, M. Iizuka, K. Minami, S. Tejima, and H. Nakamura, Phys. Rev. B **71**, 134515 (2005).
[11] S. Savel'ev, A. L. Rakhmanov, and F. Nori, Phys. Rev. B **74**, 184512 (2006).
[12] M.-H. Bae, H.-J. Lee, and J.-H. Choi, Phys. Rev. Lett. **98**, 027002 (2007).
[13] R. Kleiner, F. Steinmeyer, G. Kunkel, and P. Müller, Phys. Rev. Lett. **68**, 2394 (1992).
[14] G. Oya, N. Aoyama, A. Irie, S. Kishida, and H. Tokutaka, Jpn. J. Appl. Phys., Part 2 **31**, L829 (1992).
[15] Y.-J. Doh, J. Kim, K.-T. Kim, and H.-J. Lee, Phys. Rev. B **61**, R3834 (2000).
[16] M. H. Bae, R. C. Dinsmore, M. Sahu, H. J. Lee, and A. Bezryadin, Phys. Rev. B **77**, 144501 (2008).
[17] R. L. Kautz, J. Appl. Phys. **52**, 6241 (1981).
[18] A. E. Koshelev and I. S. Aranson, Phys. Rev. Lett. **85**, 3938 (2000); Phys. Rev. B **64**, 174508 (2001).
[19] T. Koyama and M. Tachiki, Phys. Rev. B **54**, 16183 (1996).
[20] Yu. I. Latyshev, A. E. Koshelev, and L. N. Bulaevskii, Phys. Rev. B **68**, 134504 (2003).
[21] R. L. Kautz, Appl. Phys. Lett. **36**, 386 (1980).
[22] In Ref. 7 stability of the synchronized state with respect to $n$-dependent perturbations homogeneous in $y$ direction has been demonstrated. It is straightforward to include $y$-dependent perturbations in this analysis for very long mesas, $w \gg \lambda_\omega$, which can be treated as infinite in $y$ direction. For shorter mesas, we analyzed the stability of the synchronized state in a system shown in Fig. 1 with a simplifying modification, assuming that additional screens are placed to the right and to the left from the crystal, i.e., at $|y| > w/2 + d$ and $|x| < L_x/2$. Here $d \ll \lambda_\omega$ is small distance between screens and crystal edges to avoid shortage of crystal layers. We found that the conditions of stability are almost the same as those derived in Ref. 7, i.e., the radiation field and weak dissipation result in synchronization of Josephson oscillations in different layers and along the $y$ axis.
[23] M. T. Levinsen, M. J. Feldman, and B. A. Tucker, Appl. Phys. Lett. **31**, 776 (1977).